

Surface properties of exotic isotopic chains using relativistic mean-field formalism

A Dissertation

*Submitted in Partial Fulfillment of the Requirement for the Award of
Degree of*

**Master of Science
In
Physics**

Submitted By:

Praveen Kumar Yadav

Roll No. 301904013

Under the supervision of:

Dr. Raj Kumar

Assistant Professor

T.I.E.T. Patiala



THAPAR INSTITUTE
OF ENGINEERING & TECHNOLOGY
(Deemed to be University)

SCHOOL OF PHYSICS AND MATERIALS SCIENCE
THAPAR INSTITUTE OF ENGINEERING AND TECHNOLOGY, PATIALA
PUNJAB-147004
JUNE-2021

*Dedicated to my Family
and my Mentors.*

Declaration

I hereby declare that the dissertation entitled “**Surface properties of exotic isotopic chains using relativistic mean-field formalism**” is an authentic record of my work carried out as a requirement for the award of the degree of **Master of Science** at **Thapar Institute of Engineering and Technology, Patiala, India** under the supervision of **Dr. Raj Kumar**, Assistant Professor, School of Physics and Materials Science, Thapar Institute of Engineering and Technology, Patiala, India.

This work has been done in collaboration with **Dr. Mrutunjaya Bhuyan**, Senior Lecturer, Universiti Malaya, Kuala Lumpur, Malaysia.

No part of the matter embodied in this dissertation has been submitted to any other university or institute for the award of any degree.



Dated: 30/07/2021

(**Praveen Kumar Yadav**)

301904013

It is certified that the above statement made by the student is correct to the best of my knowledge and belief.



(**Dr. Raj Kumar**)

Supervisor

Assistant Professor
SPMS, TIET, Patiala

Acknowledgment

I wish to acknowledge with a most heartfelt sense of gratitude for the opportunity and valuable guidance rendered on me by **Dr. Raj Kumar**, Assistant Professor, Thapar Institute of Engineering and Technology, Patiala, India. I am incredibly thankful to him for his humility to take me as his student, believing in me to undertake the problem I was given during this work and giving me the flexibility and liberty to carry out this work. I pour my special and sincere gratitude towards **Dr. Mrutunjaya Bhuyan**, Senior Lecturer, University of Malaya, Kuala Lumpur, Malaysia for his constant support and his knowledge about the subject.

I am also grateful to the University of Malaya, Kuala Lumpur, Malaysia for the facility and resources provided during the progression of this work.

I am highly obliged to **Prof. O. P. Pandey**, Head, School of Physics and Materials Science for his support. I want to embrace this opportunity to acknowledge my gratitude towards all the faculty members of the School of Physics and Materials Science who were always accessible and helpful.

I am deeply grateful to my parents and my elder brother for showering their blessings and encouraging me to follow my dream of pursuing a research career in nuclear astrophysics. I am also thankful to my friends for their constant support and boosting my morale.



(Praveen Kumar Yadav)

List of Publications arising from the thesis

Journals

1. “Isospin dependent properties of the isotopic chain of Scandium and Titanium nuclei within the relativistic mean-field formalism”, **Praveen K. Yadav**, Raj Kumar, M. Bhuyan, Chinese Physics C (Communicated).
2. “Relevance of infinite nuclear matter quantities in finite nuclei”, **Praveen K. Yadav**, Raj Kumar, M. Bhuyan, Student Journal of Physics (Communicated).

Conferences

1. “Effect on symmetry energy at shell/sub-shell closure within relativistic mean-field formalism”, **Praveen K. Yadav**, Raj Kumar, M. Bhuyan, DAE Symposium on Nuclear Physics **65** (2021).
2. “Isospin asymmetry properties in exotic nuclei: A signature of shell/sub-shell closure”, **Praveen K. Yadav**, Raj Kumar, M. Bhuyan, 1st International Symposium On Recent Advances In Fundamental And Applied Sciences **1284** (2021), pp. 71, 343-347.

Contents

List of Figures	vi
List of Tables	vii
Abstract	viii
1 Introduction and Literature Review	1
1.1 Introduction	1
1.2 Nuclear landscape	2
1.2.1 Proton-rich nuclei	3
1.2.2 Neutron-rich nuclei	4
1.2.3 Nuclear drip-line	4
1.2.4 Exotic and halo nuclei	5
1.2.5 Nuclear deformations	6
1.3 Theoretical nuclear models	6
1.3.1 Effective field theory	7
1.4 Plan of the thesis	9
2 Methodology	10
2.1 Basic concepts of relativistic mean-field theory	10
2.1.1 Relativistic mean-field Lagrangian density	12
2.2 Relativistic mean-field equations	15
2.3 Coherent density fluctuation method	17
2.4 Developing the Fortran program	19
3 Results and discussions	23
3.1 Densities and weight function	23
3.2 Nuclear symmetry energy	25
4 Summary and conclusions	30
4.1 Brief summary	30
4.2 Future scope of the project	31

List of Figures

1.1	Nuclear landscape showing different stable nuclei and their decay modes [1].	3
2.1	The qualitative structure of the Lorentz scalar field S and the vector field V in finite nuclei. Here M_N and M_N^* are the nucleon masses and effective nucleon masses, respectively. The $S+V$ represents Dirac positive energy and $-S+V$ represents Dirac negative energy [2].	16
3.1	Total density distribution for $^{57}\text{Sc}(\text{NL3})$ and $^{35}\text{Sc}(\text{DDME2})$ isotopes. . . .	24
3.2	Total density distribution for $^{56}\text{Ti}(\text{NL3})$ and $^{40}\text{Ti}(\text{DDME2})$ isotopes . . .	25
3.3	The weight function distribution calculated for $^{57}\text{Sc}(\text{NL3})$ and $^{35}\text{Sc}(\text{DDME2})$ isotopes.	26
3.4	The weight function distribution calculated for $^{56}\text{Ti}(\text{NL3})$ and $^{40}\text{Ti}(\text{DDME2})$ isotopes.	27
3.5	The symmetry energy for Scandium isotopes with respect to neutron number for the NL3 and DD-ME2 interactions. More details are provided in the text.	28
3.6	The symmetry energy for Titanium isotopes as a function of number of neutrons for the NL3 and DD-ME2 parameters. Detailed explanation is provided in the text.	29

List of Tables

- 2.1 Classification of different meson based on their associated quantum number 11

Abstract

The density-dependent nuclear symmetry energy (NSE) characterizes the variation of the binding energy with the change in the isospin asymmetry (ratio of the number of neutrons to that of protons). The NSE and its related observables play a crucial role in understanding the various branches of nuclear physics and astrophysics, such as analyzing the nuclear structure of exotic nuclei, dynamics of heavy-ion collision, supernova explosion, and neutron stars study. In this theoretical work, we study the density-dependent isospin properties of finite nuclei of *odd - A* isotopes of Scandium ($Z = 21$) and *even - even* isotopes of Titanium ($Z = 22$) for non-linear NL3 and density-dependent DD-ME2 parameters within the relativistic mean-field formalism. Using the coherent density fluctuation method, we calculate the weight function. Moreover, we investigate the symmetry energy as a function of the neutron number along the isotopic chain of Scandium and Titanium nuclei. This theoretical approach opens new avenues in understanding and predicting newer magicity along the drip-line and the nuclear landscape as a whole.

Chapter 1

Introduction and Literature Review

1.1 Introduction

The discovery of the nucleus marked the start of a new era in studying nuclear physics. Before that, many theoretical models of atoms were proposed, of which the most significant one was the “Plum pudding model” by J.J. Thomson, which, although described the charge neutrality of the atom, failed to mention anything about the nucleus. Later on, in 1911, the famous gold foil α -particle scattering experiment was performed by Rutherford, which revealed the existence of a nucleus inside an atom. It proposed that the mass of an atom is primarily concentrated in the central region called a nucleus, beyond which large empty space is present. Later on, it was realized that for many nuclei, the atomic mass number (A) is slightly greater than twice that of the proton number (Z). This led to a newfound interest in understanding the nuclear structure. In 1932, Landau published a paper that speculated on the existence of neutron stars. In the same year, J. Chadwick used the data observed in the bombardment of α -particle on beryllium (${}^9\text{Be}$) to concur the existence of neutral particles called as neutrons. During that time, owing to the nature of charge independence of nuclear force, nucleon-nucleon interactions were not taken into account.

In 1935, Yukawa, through his pioneering work on meson theory, suggested that massive mesons or bosons act as a mediator for nucleonic interactions. He postulated that π -meson, which has a mass of about 140 MeV, accounts for the residual force between the nucleons and that the muons with a mass of 105.66 MeV do not take part in strong nuclear interactions. The existence of muons was finally confirmed experimentally in 1937. Later

in 1947, C.F.Powell and his team successfully discovered the existence of π -mesons in the interaction of cosmic-ray particles. Soon after, a race began to find newer, heavier particles in different laboratories, which resulted in the discovery of ρ , ω , and δ mesons.

Naturally, about 300 nuclei are found in existence, and about 300 nuclei are synthesized by Radioactive Ion Beam (RIB) facilities, and various models predict more than 5000 more nuclei. Recently element Oganesson ($Z = 118$) was discovered and was placed in the periodic table of elements. The properties of the nuclei that are naturally occurring and long-lived are well studied. In contrast, artificial nuclei with abnormal characteristic properties are located far away from β -stability valley. These nuclei are known as exotic nuclei and will be further discussed in subsequent sections. In the present thesis, we perform a detailed study on the surface properties of exotic nuclei. Before venturing any further, we list some of the important general concepts related to nuclear structures.

1.2 Nuclear landscape

For more than a century, nuclear physicists have been trying to figure out the nature of stability in nuclei across the nuclear landscape. The nucleus is an essential component of an atom comprising the entire mass of the element. The nuclear force existing between the nucleons present inside the nucleus constitutes a substantial chunk of study taking place in nuclear and particle physics. Among the many problems, the nuclear physicist's central dilemma is finding the answer to how many protons and neutrons produce a stable nucleus. Based on different observations, the stable elements that exist in nature have a half-life in the same order as the earth. Approximately 300 naturally occurring nuclei have been discovered to have a half-life equal to or greater than that of the earth. These stable nuclei are also referred to as β -stable nuclei.

The nuclear landscape is represented in Fig. 1.1. The black boxes depict different stable nuclear isotopes. From the figure, one can note that with the increase in mass number, the number of neutrons in stable isotopes also increases. Newly discovered and yet unknown isotopes of various elements are also represented in the figure. Many theoretical as well as experimental research, is being conducted to account for the existence of these nuclei. The advent of the RIB (RIB) during the 1980s ushered in a new era in exploring new isotopes away from the line of β -stability. Various experimental groups

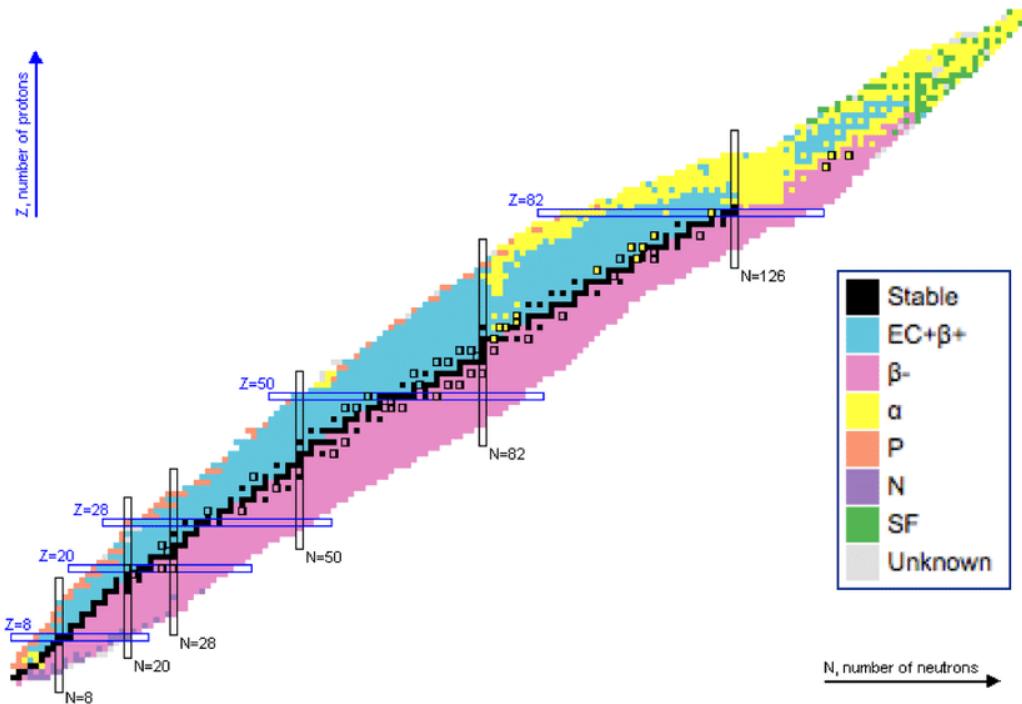


Figure 1.1: Nuclear landscape showing different stable nuclei and their decay modes [1].

from RIKEN (Japan) [3], ORNL and FRIB (US) [4, 5], Jyväskylä (Finland) [6], FAIR and GSI (Germany) [7, 8], CSR (China) [9], GANIL (France) [10] and FLNR (Russia) [11] are running various studies related to exotic nuclei which under extreme settings have large values of isospin asymmetry. In these facilities, around 2000 artificial isotopes that are naturally unstable have been synthesized. Based on various theoretical models, nearly 5000 more isotopes may be explored in the foreseeable future.

1.2.1 Proton-rich nuclei

In the nuclear landscape, only a small fraction of exotic nuclei exhibit the proton-rich characteristic. In these nuclei, the repulsion occurring due to Coulombic interactions between protons hinders the possibility of the existence of such nuclei. Beyond iron, the majority of naturally occurring nuclides can be created in either of the two methods: firstly using the slow neutron-capture process, also known as the s-process, and secondly using the fast neutron-capture process, also known as the r-process. The (p, γ) or (γ, n) processes are widely used to create proton-rich nuclei. The first process involves the repeated proton addition, whereas the second process involves the photo-disintegration of neutrons done sequentially, resulting in the formation of nuclei having the proton-rich

characteristic.

1.2.2 Neutron-rich nuclei

The r-process and s-process are also primary mechanisms for creating neutron-rich nuclei. About half of the proton-rich elements that are heavier than iron can be created using the r-process. The s-process leads in situations with a low density of neutrons and intermediate temperature, paving the way for the formation of heavier nuclei using the neutron capture method, which is done by incrementing a single unit of atomic weight for each nucleus. This process involves converting neutron to proton to form a daughter nucleus with a higher atomic number, which entails a slower neutron capture rate in contrast to the rate of β -decay. Alternatively, β -decay and s-process can happen directly before each consecutive neutron capture process. Therefore, in the nuclear landscape, while moving across the valley of β -stable isobars, although the r-process is known to have a faster rate of neutron capture than the β -decay, the s-process yields stable isotopes. In the case of the r-process, more than one neutron is captured before the occurrence of β -decay process. Moreover, this process is employed in thermonuclear weapon explosions and is responsible for discovering many elements, namely Einsteinium ($Z = 99$), Fermium ($Z = 100$), etc.

1.2.3 Nuclear drip-line

Theoretically, the current estimate of bound nuclei through strong nuclear force is nearly 6000. However, approximately 2000 of these nuclei are observed at present. It is found that beyond a certain number of nucleons, the separation energy of neutron S_n and proton S_p becomes zero, which concurs that the nucleus is unbound. This point where $S_n=0$ is known as the neutron drip-line, and the point where $S_p=0$ is known as the proton drip-line. Therefore, on the nuclear landscape, the drip-line can be defined as the final boundary away from the β -stability line beyond which no extra neutrons or protons can be added. The neutron and proton drip-lines are represented in Fig. 1.1.

It is worth noting that the drip-line is well-defined till oxygen. However, the ^{23}O and ^{24}O nuclei are found to be unbound in their ground state. Moreover, the unbound states of ^{26}O and ^{28}O are found to have a double closed shell with *even – even* stability. The possibility of ^{34}Ne and ^{37}Na nuclei, which were predicted to be unstable, were discovered

in various experiments at GANIL [12] as well as at RIKEN [13]. The recent discovery of ^{42}Al and ^{40}Mg [14], both of which are far beyond the drip-line according to numerous mass formulas, directly contradicts the results of various theoretical models for a well-defined neutron drip-line.

The effective nucleonic interaction dependence on isospin is not fully understood. As the ratio of N/Z increases significantly, the uncertainty in finding single-particle states structure, collective modes and global nuclear properties increases. In recent years, various experimental and theoretical studies are conducted to study the nuclei closer to the drip-line. These theoretical and experimental studies have revealed the existence of different magic numbers than what is observed in the valley of β -stable nuclei [15–17]. More research is needed to understand the appearance and disappearance of magic numbers in nuclei near the proton or neutron drip-line.

1.2.4 Exotic and halo nuclei

When compared to surrounding isotopes, several nuclear systems exhibit anomalous behavior. One of the extraordinary property of exotic nuclei is its extreme neutron to proton ratio (can be very high or very low) which leads to high instability and are very quick to decay into stable nuclei. That is why these nuclei are located far away from the line of β -stability. After decay, the nucleus becomes highly excited and can emit one or more particles of protons, neutrons, or an α -particle in β -delayed emission.

Such nuclei, while exhibiting strange properties, test the limits of conventional models. The study of nuclear matter (NM) at such extreme conditions that the nucleus acts much differently than in stable nuclear systems is crucial in understanding explosive astrophysical phenomena, namely, supernovae and stellar core collapse. The phenomena of halo in the exotic nucleus was discovered in 1985 [18, 19]. Generally, in halo nucleus, the individual nucleons lie far away from the core of the nucleus. Some of the most studied neutron-halo nuclei includes ^6He , ^{11}Li and ^{11}Be . The variation in the nuclear charge distribution of neutron-halo nucleus provides insight into the interactions of various sub-systems of the strong clustered nucleus. These changes can be accounted for from the nuclear correlative motion to that of the center of mass and induced core polarization due to the interaction between the core and the neutron-halo. These nuclei, apart from having extremely high or low N/Z values, show high density and temperature. It is worth

noting that the nuclear shapes and effects of deformations are crucial in understanding the nature of an exotic nuclear system.

1.2.5 Nuclear deformations

In the case of a deformed nucleus, large electrical quadrupole moments can be obtained through the contribution of many protons. The nuclear deformation can be observed due to the polarizing effect of either one or more loosely bounded nucleons on the rest of the nucleus. The concept of magic number was first explained using the spherical shell model, which considers the Pauli exclusion principle. The nuclei with magic shell configuration in their proton numbers and or neutron numbers have spherical shell configuration and, thus, higher stability than those with non-magic shells. Recent experimental results related to mass and Coulomb excitation measurements obtained from RIB for neutron-rich isotopes of Na ($Z=11$) and Mg ($Z=12$) imply splitting of the nuclear shell near $N = 20$. Moreover, studying the neutron separation energy (S_n) near the drip-line and various cross-section measurements for the shells of p-sp and sd reveals the existence of $N = 16$ as a new magic number [20, 21]. Recent RIB experiments at RIKEN [16] on exotic nuclei predicts some newer magic numbers, namely $N = 6, 16, 34$, etc., which violates the traditional order of nuclear magicity. The disappearance of recognized shell gaps and the emergence of novel stability zones results in a combination of both normal and intruder configurations, which has a profound effect on the various properties of these nuclei [15, 22]. Advancements in the shell model have provided the concept of deformed magic numbers, which are so named as they are found to stabilize nucleus having deformed shaped configuration [20, 21, 23].

1.3 Theoretical nuclear models

The atomic nucleus can be defined as a strongly interacting, quantum mechanical system with many-body having a wide variety of spherical and super-deformed shapes and excitation modes. Another intriguing aspect of the nucleus is the excitation of a single proton or neutron to collective rotations and vibrations of nucleons. The primary objective of nuclear physicists is to investigate these complicated patterns of nuclear behavior using a single technique. The different aspects related to the nuclear structure are

investigated using nuclear bulk parameters, namely binding energy, *rms* radius, charge radius, deformation parameter, etc. Various phenomenological as well as microscopic theoretical models, namely the Finite Range Droplet Model [24], Skyrme Hartree-Fock [25, 26], Relativistic Mean Field [27, 28], and Hartree Fock Bogulibov model [29, 30] have been developed through research of these features. Moreover, the ab-initio method was introduced in order to provide an explanation related to data on nuclear scattering using the nucleon-nucleon potential. This method considers the NM as a correlated quantum liquid owing to the extreme repulsive potential of the nucleus core. Such a complex system requires many-body theories that are very sensitive [31, 32] and thus may provide a direct link between the two-nucleon problem and the properties of nuclear matter.

1.3.1 Effective field theory

The self-consistent Effective Field Theory (EMF) models successfully explained many phenomena in nuclear-astrophysics, which includes the properties related to finite nuclei as well as extreme supra-normal densities [33, 34]. Different laboratories across the world are experimenting to define the limit of the neutron-proton ($N - P$) drip-line. Recently, various nuclear phenomena within the purview of relativistic and non-relativistic formalism have been theoretically predicted near the neutron drip-line. The RMF theory has turned out to be the most successful self-consistent effective formalism for describing various nuclear phenomena.

It may be noted that, even though the energy density functional for both the RMF as well as non-relativistic models are different, the results obtained for finite nuclei, for the most part, are nearly the same. RMF has also accounted successfully for all the valid properties of nuclear matter at extremely high densities, such as the neutron stars. In RMF, mesons exchange is used to describe the interactions among the nucleons, where mesons are collectively taken as effective fields represented by classical numbers. Succinctly, RMF model is the relativistic Hartre-Fock approximation to that of one-boson exchange theory, which involves the interaction of nucleons with one other through the exchange of isovector δ -, ρ - and π - mesons as well as isoscalars ω - and η - mesons. The η - and ω - mesons come under the class of pseudo-scalar, which neither contribute to the properties of ground-state of even nuclei nor do they follow the parity symmetry of ground-state.

A simple relativistic Lagrangian accounts for the contributions of the ρ -, σ - and ω -mesons without including any of the non-linear term. However, this model, when implemented for the infinite nuclear matter, has a large error in the value of compressibility K at saturation. In order to lower this error to be an acceptable level, Boguta and Bodmer [35] instated the self-coupling terms in the case of σ mesons. Following this, large sets of parameters, namely NL1 [36], NL2[36], NL3[37] as well as NL3*[38] were updated. The prediction quality of the properties of finite nuclei and incompressibility was successfully improved to a large extent with the addition of self-coupling terms of σ mesons. At the same time, the EOS at supra-normal densities is observed to be rather stiff. Therefore, different parameter sets were constructed to account for the self-coupling vector mesons in the Lagrangian density, which largely explained the nuclear matter and finite nuclei [18, 23]. It was observed that the non-relativistic model's EOS fails to reach to the Coester-band or empirical saturation point of symmetric NM (at $\rho_0 \simeq 0.16 \text{ fm}^{-3}$ the $E/A \simeq -16.0 \text{ MeV}$). Moreover, it was later found that at extreme density, like in the case of a neutron star, the results of all the models showed large dissimilarity in nature. Eventually, it was later theorized to have different strategies to mitigate this issue by designing coupling constants that are density-dependent and the theory of effective mean-field formalism (E-RMF). Many free parameters are accounted in the energy-density functional, and their values are fitted to empirical and experimental data.

These values are calculated using constraints derived from:

- Experimental finite nuclei observations that are based on static properties such as binding energy and charge radius.
- Nuclear matter's characteristic properties include binding energy, saturation density, charge radius and symmetry energy.
- Dipole resonances and giant monopole excitations.
- Mass and radius observations on a dense astrophysical matter such as neutron stars and supernovae.

1.4 Plan of the thesis

We have summarized the contents of the following chapters in this section. The entire effort is devoted to developing an understanding of novel theories that can explain the structural properties of drip-line nuclei within the RMF model. The thesis is organized as follows:

After the introduction, in chapter 2, we outline the basic concepts related to RMF. We derive the expression for E-RMF Lagrangian which includes cross-coupling as well as δ meson along with the equation of motion (EOM) for various fields such as ϕ , σ , ω , ρ , δ and EM field. We then study the coherent density fluctuation method (CDFM), a natural extension of the Fermi-gas model. This method is based on the limit of δ -function of the generator coordinate. Moreover, we present the procedure of drafting a Fortran program that is capable of calculating weight function $|\mathcal{F}(x)|^2$ as well as nuclear symmetry energy (NSE) from an input file containing the values of total density corresponding to the nuclear distance.

In chapter 3, we present the theoretical result of our calculations of $|\mathcal{F}(x)|^2$ corresponding to the nuclear distance (r). We then calculate the symmetry energy as a function of N with NL3 and DD-ME2 parameter sets for *odd - A* Scandium ($Z = 21$) isotopes and *even - even* Titanium ($Z = 22$) isotopes within the RMF formalism. We have predicted some shell and or sub-shell closure for low-mass isotopic chains of nuclei.

Finally, in chapter 4, a brief summary and future prospects are discussed.

Chapter 2

Methodology

During the 1960s, Schiff [39], Johnson and Teller [40] along with Durr [41] put forward the concept of a relativistic nuclear system. Later through the work of J.D. Walecka [42], a simple form of nucleonic interaction was proposed. This model involves renormalizability which creates issues owing to significant effects obtained from loop integrals that accounts for the dynamics related to quantum vacuum. The relativistic mean-field (RMF) model is known to provide far better predictions for exotic nuclei that lie far away from the valley of β -stability. Some general concepts related to the RMF model are discussed in the following section.

2.1 Basic concepts of relativistic mean-field theory

In recent years, RMF theory has been used to provide a microscopic account of the ground state as well as excitation properties related to finite nuclei. This model involves many-body, which in the initial phase considers Effective Lagrangian with different nucleonic and mesonic degrees of freedom. Table 2.1 categorizes various meson with their corresponding quantum numbers.

The basic assumptions of RMF theory are as follows:

- Nucleons are regarded as point particles that are included in the form of Dirac spinors ψ_i . This is because at low energies, they can be expressed as efficient degrees of freedom. Moreover, by taking into account interaction involving non-renormalizable terms, their compositeness is well-preserved at the tree level.
- These particles do abide by the laws of causality and relativity. Moreover, this

Table 2.1: Classification of different meson based on their associated quantum number

Type	Spin S	Orbital angular moment L	Parity P	Total angular moment J
Pseudoscalar	0	0	−	0
Pseudovector	0	1	+	1
Vector	1	0	−	1
Scalar	1	1	+	0
Tensor	1	1	+	2

formalism is Lorentz invariant.

- In RMF, the particles travel freely in mean fields that are created by the interactions of nucleon-nucleon.
- The Non-Goldsten mesons/bosons namely, ρ , δ , ω , and σ are incharge of interactions at intermediate range as they express the nuclear bi-linear successfully in terms of non-zero expectation values.
- The constraints of Quantum Hydrodynamics are put forward via symmetry, which requires the inclusion of all permissible terms.

The effective mesons transfer that couple to nucleon's local vertices follows Lorentz invariance and the causality criteria. These assumptions lead to nucleons being characterized as the Dirac particles with Dirac spinor ϕ_i . Mesons ϕ_j are point-like particles, where j represents the ρ -, σ -, δ -, ω - as well as photon fields. The quantum numbers of these mesons are given in terms of spin, total angular momentum and parity. The dynamics of mesons can be derived from Lagrangian density as:

$$\delta \int dt L = \delta \int d^4x \mathcal{L}(\phi, \partial_\mu \phi, t) = 0. \quad (2.1)$$

In terms of classical Euler-Lagrange EOM we have,

$$\partial_\mu \left(\frac{\partial \mathcal{L}}{\partial(\partial_\mu \phi_j)} \right) - \frac{\partial \mathcal{L}}{\partial \phi_j} = 0 \quad (2.2)$$

Following Ref. [32, 35] the energy-momentum tensor can be described as

$$T^{\mu\nu} = -g^{\mu\nu}\mathcal{L} + \left(\frac{\partial\mathcal{L}}{\partial(\partial_\mu\phi_j)}\right)\partial^\nu\phi_j. \quad (2.3)$$

From the continuity equation we have

$$\partial_\mu T^{\mu\nu} = 0. \quad (2.4)$$

If there exist no space dependence explicitly of \mathcal{L} , then the four-momentum vector can be stated as $P^\nu = \int d^3r T^{0\nu}$. Here the 0^{th} component of our four-momentum vector can be given as $P^0 = E = \int d^3r \mathcal{H}(r)$.

The expression of Hamiltonian density, as well as binding energy, can be given as

$$\mathcal{H}(r) = T^{00} = \frac{\partial\mathcal{L}}{\partial q_j}\phi_j - \mathcal{L}. \quad (2.5)$$

$$E = \int d^3r \mathcal{H}(r) = \int T^{00} d^3r. \quad (2.6)$$

In mean-field formalism, accurate values of parity are obtained. Hence, while it describes bulk nuclear properties, the average π - mesons interactions effects turn out to be zero [32, 35]. It may be noted that an even number of pions contributes positive parity and thus is required to incorporate the phenomenological resonance states of two π -mesons called σ -mesons that are beyond mean-field.

2.1.1 Relativistic mean-field Lagrangian density

Using all the mesonic and nucleonic contributions, the effective Lagrangian non-linear density can be used to explore the ground state properties of the nuclei. It can thus be described as:

$$\mathcal{L} = \mathcal{L}_N + \mathcal{L}_M. \quad (2.7)$$

Here \mathcal{L}_N and \mathcal{L}_M are respectively the nucleonic part and the mesonic part of the Effective Lagrangian.

$$v = d + \frac{n}{2} + b. \quad (2.8)$$

Each term is approximated up to $\nu = 4$, which helps in evaluating finite as well as infinite nuclear matter [43, 44]. Here ‘n’, ‘b’ and ‘d’ are the number of nucleon fields, non-Goldstone boson field, and a number of derivatives, respectively, in the interactions.

The first term of the Effective Lagrangian for nucleon having $\nu = 4$ is stated below.

$$\begin{aligned} \mathcal{L} = & \bar{\psi}_i [i\gamma^\mu D_\mu + g_A \gamma^\mu \gamma_5 a_\mu - M + g_s \phi] \psi_i \\ & - \frac{f_p g_p}{4M} \bar{\psi}_i \rho_{\mu\nu} \sigma^{\mu\nu} \psi_i - \frac{f_\omega g_\omega}{4M} \bar{\psi}_i V_{\mu\nu} \sigma^{\mu\nu} \psi_i \\ & - \frac{k_\pi}{M} \bar{\psi}_i \omega_{\mu\nu} \sigma^{\mu\nu} \psi_i - \frac{e}{2M} F_{\mu\nu} \bar{\psi}_i \lambda \sigma^{\mu\nu} \psi_i \\ & - \frac{e}{2M} \bar{\psi} \gamma_\mu (\beta_s + \beta_v \tau_3) \psi_i \partial_\nu F_{\mu\nu}. \end{aligned} \quad (2.9)$$

Here ψ_i is known as Dirac spinors and D_μ is known as covariant derivative which is defined as

$$D_\mu = \partial_\mu + i\omega_\mu + ig_\rho \rho_\mu + ig_\omega V_\mu + \frac{ieA_\mu(1 + \tau_3)}{2} \quad (2.10)$$

In the Lagrangian given in Eq. 2.7 the meson part may be rewritten using various

fields along with their derivatives in the form:

$$\begin{aligned}
 \mathcal{L}_{\mathcal{M}} = & \frac{1}{2} \left[1 + \alpha_1 \frac{g_s \phi}{M} \right] \partial_\mu \phi \partial^\mu \phi + \frac{f_\pi^2}{4} \text{tr} \left(\partial_\mu U \partial^\mu U^\dagger \right) \\
 & - \frac{1}{2} \text{tr} (\rho_{\mu\nu} \rho^{\mu\nu}) - \frac{1}{4} \left[1 + \alpha_2 \frac{g_s \phi}{M} \right] V_{\mu\nu} V^{\mu\nu} - g_{\rho\pi\pi} \frac{2f_\pi^2}{m_\rho^2} \text{tr} (\rho_{\mu\nu} \rho^{\mu\nu}) \\
 & + \frac{1}{2} \left[1 + \eta_1 \frac{g_s \phi}{M} + \frac{\eta_2 g_s^2 \phi^2}{2 M^2} \right] m_\omega^2 V_\mu V^\mu + \frac{1}{4!} \zeta_0 g_\omega^2 (V_\mu V^\mu)^2 \\
 & + \left[1 + \eta_\rho \frac{g_s \phi}{M} \right] m_\rho^2 (\rho_\mu \rho^\mu) - m_s^2 \phi^2 \left[1 + \frac{\kappa_3 g_s \phi}{3! M} + \frac{\kappa_4 g_s^2 \phi^2}{4! M^2} \right] \\
 & - 2e f_\pi^2 A^\mu \text{tr} (\omega_\mu \tau_3) - \frac{e}{2g_\gamma} F_{\mu\nu} \left[\text{tr} (\tau_3 \rho^{\mu\nu}) + \frac{1}{3} V^{\mu\nu} \right].
 \end{aligned} \tag{2.11}$$

In the above equation, photons, ω -, ρ -, and σ - mesons have the coupling constants $\frac{e}{4\pi} = \frac{1}{137}$, g_ω , g_ρ and g_σ respectively. For the nucleon spinors, it is possible to define Pauli isospin matrix as $\vec{\tau}_3$, where $\vec{\tau}_3$ is defined as the third component of τ . One may note that for neutron and proton, τ_3 can have value either +1 or -1. For the case of non-linear terms of meson fields, the coupling constant $\eta_1, \eta_2, \eta_\rho$ and ζ_0 are also induced. The field tensors $\rho^{\mu\nu}$, $V^{\mu\nu}$ and $F^{\mu\nu}$ corresponds to the ρ and ω mesons along with EM field respectively. Moreover, the terms α_1 and α_2 are the derivative for meson field where $\nu = 5$.

A generalized relativistic \mathcal{L} (Lagrangian density) with certain changes implemented to the original Walecka \mathcal{L} accounts for various limitations for the many-body meson-nucleon systems that take the form as:

$$\begin{aligned}
 \mathcal{L} = & \bar{\psi} \{ i\gamma^\mu \partial_\mu - M \} \psi + \frac{1}{2} \partial^\mu \sigma \partial_\mu \sigma \\
 & - \frac{1}{2} m_\sigma^2 \sigma^2 - \frac{1}{3} g_2 \sigma^3 - \frac{1}{4} g_3 \sigma^4 - g_s \bar{\psi} \psi \sigma \\
 & - \frac{1}{4} \Omega^{\mu\nu} \Omega_{\mu\nu} + \frac{1}{2} m_\omega^2 \omega^\mu \omega_\mu - g_\omega \bar{\psi} \gamma^\mu \psi \omega_\mu \\
 & - \frac{1}{4} \vec{B}^{\mu\nu} \cdot \vec{B}_{\mu\nu} + \frac{1}{2} m_\rho^2 \vec{\rho}^\mu \cdot \vec{\rho}_\mu - g_\rho \bar{\psi} \gamma^\mu \vec{\tau} \psi \cdot \vec{\rho}^\mu \\
 & - \frac{1}{4} F^{\mu\nu} F_{\mu\nu} - e \bar{\psi} \gamma^\mu \frac{(1 - \tau_3)}{2} \psi A_\mu.
 \end{aligned} \tag{2.12}$$

The vector field tensors defined in the above Lagrangian density can be stated as

$$\begin{aligned}
 F^{\mu\nu} &= \partial_\mu A_\nu - \partial_\nu A_\mu \\
 \Omega_{\mu\nu} &= \partial_\mu \omega_\nu - \partial_\nu \omega_\mu
 \end{aligned}$$

$$\vec{B}^{\mu\nu} = \partial_\mu \vec{\rho}_\nu - \partial_\nu \vec{\rho}_\mu. \quad (2.13)$$

Here the fields for the various ω , σ and isovector ρ meson is denoted by ω_μ , σ and $\vec{\rho}_\mu$ respectively. Moreover, the EM field is represented in terms of A_μ . The $F^{\mu\nu}$, $\Omega^{\mu\nu}$, and $\vec{B}_{\mu\nu}$ corresponds to field tensors for the photon fields, ω^μ , and $\vec{\rho}_\mu$ respectively.

The RMF theory allows density dependence of coupling of nucleon-meson. The mesons coupling to the nucleon fields is stated as:

$$g_i(\rho) = g_i(\rho_{sat}) f_i|_{i=\sigma,\omega}, \quad (2.14)$$

where

$$f_i(x) = a_i \frac{1 + b_i(x + d_i)^2}{1 + c_i(x + d_i)} \quad (2.15)$$

and

$$g_\rho = g_\rho(\rho_{sat}) e^{a_\rho(x-1)}. \quad (2.16)$$

Here, we find eight real parameters along with $x = \rho/\rho_{sat}$ that are related to one another. Moreover, decrement in the different number of independent parameters due to the five constraints namely, $f_i(1) = 1$, $f''_\omega(1) = f''_\sigma(1)$ and $f'_i(0) = 0$, leads decrement in effective parameters to three as given in Refs.[35, 45–48]. By extending the upper as well as lower components of the boson fields and Dirac spinors in a harmonic oscillator that has an axially deformed configuration basis with the initial deformation β_0 , we can find the field equations for respective nucleons and mesons using the aforementioned Lagrangian density.

2.2 Relativistic mean-field equations

The equation of motion (EOM) for nucleons and mesons is created using the variational principle. Rather than quantizing the fields, mean-field approximations are taken into account, where the meson field operators are substituted by their classical field values, which effectively eliminates quantum fluctuations. Moreover, there exists a “no sea” approximation, having various densities and currents for the sources of meson fields that are

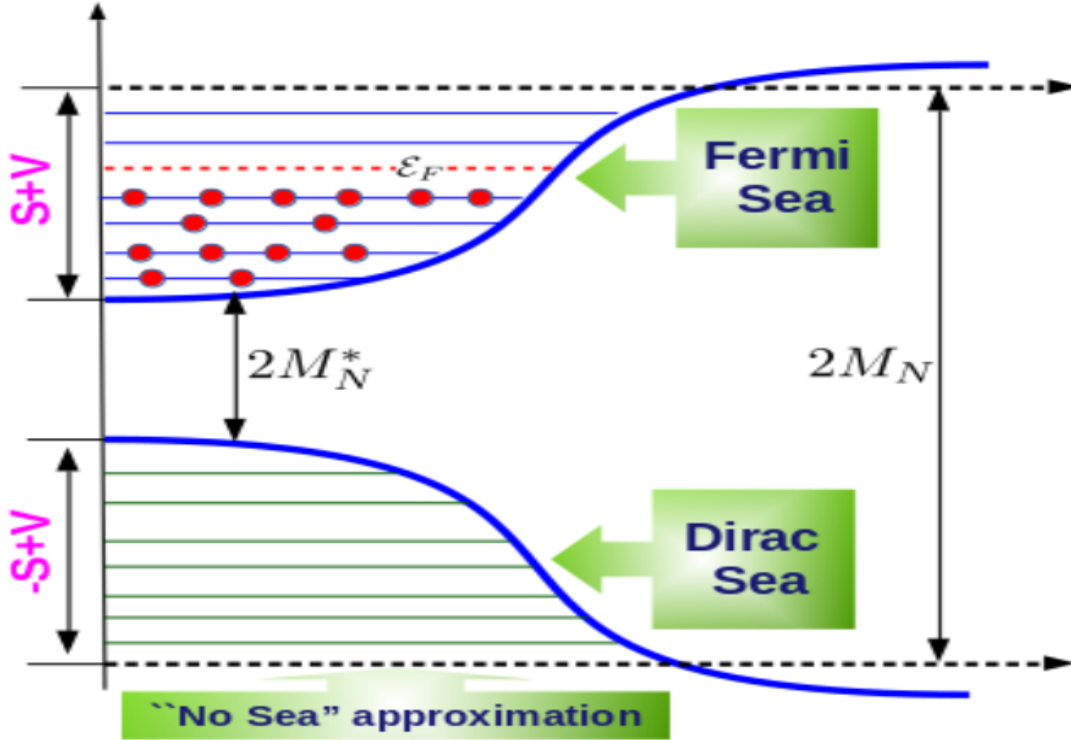


Figure 2.1: The qualitative structure of the Lorentz scalar field S and the vector field V in finite nuclei. Here M_N and M_N^* are the nucleon masses and effective nucleon masses, respectively. The $S+V$ represents Dirac positive energy and $-S+V$ represents Dirac negative energy [2].

calculated by adding different occupied states in the baryon Slater determinant, which completely overlooks contributions of anti-particle. This implies that the negative energy Dirac equation solutions or the effects of vacuum polarization are not considered. However, vacuum polarization cannot be entirely ignored, and it is required to have a phenomenological modification of the parameters that take care of it on a universal level.

In 1936, Bethe and Weizsäcker [49] successfully created the semi-empirical mass formula that has its roots in LDM, which represents different bulk properties associated with finite nuclei fairly well. Moreover, the binding energy/particle of a nucleus may be calculated using the LDM as follows:

$$\frac{E(Z, N)}{A} = M - a_v + a_s A^{-1/3} + a_c \frac{Z^2}{A^{2/3}} + a_{asym} \frac{(N - Z)^2}{A^2} + \dots \quad (2.17)$$

Here M signifies the nucleonic mass, whereas $A = Z + N$ denotes the mass number or total nucleonic number. The asymmetry, surface, volume and Coulomb terms are represented by a_{asym} , a_s , a_v and a_c respectively. If one takes Coulomb term as $a_c = 0$, and discard contribution due to surface, the LDM can be expanded to incorporate infinite

nuclear matter (INM) i.e., N, Z , as well as V achieves infinite value. As a result, the system's binding energy/nucleon can be written as

$$\begin{aligned} \frac{E(Z, N)}{A} - M &= -a_v + a_{\text{asym}} \frac{(N - Z)^2}{A^2} \\ e(\rho, \alpha) = \frac{\mathcal{E}}{\rho_B} - M &\equiv -a_v + a_{\text{asym}} \alpha^2 \end{aligned} \quad (2.18)$$

The neutron excess of INM is called the neutron-proton asymmetry in terms of baryon density which is calculated using $\alpha = (N - Z)/A = \frac{\rho_n - \rho_p}{\rho_n + \rho_p}$. Even-though, the INM is incompressible, it can be possible to expand binding energy/particle around $\alpha = 0$ for the case of compressible NM as:

$$E(\rho, \delta) = E(\rho, 0) + S(\rho)\delta^2 + O(\delta^4)\dots, \quad (2.19)$$

where δ signify isospin asymmetry. The term δ^4 signify the linear term in α becomes 0 owing to the NSE. The symmetry energy $S(\rho)$ of the system can be defined as:

$$S^{NM}(\rho) = \frac{1}{2} \left. \frac{\partial^2(\mathcal{E}/\rho)}{\partial \alpha^2} \right|_{\alpha=0}, \quad (2.20)$$

where \mathcal{E} is the energy density. In the RMF approach, we solve the field equations self-consistently by taking into account alternative inputs of the initial deformation β_0 [28, 38, 45, 47, 50, 51]. For finding converging ground state solutions in the respective region of masses, the number of main shells that will be required for fermions and bosons is given by $N_F = N_B = 12$. The mesh points obtained in Gauss-Hermite integrations is 20, while for Gauss-Laguerre integration is 24.

2.3 Coherent density fluctuation method

The CDFM is an extended version of the Fermi gas model which is established by accounting the generator coordinate. It comprises of collective type long-range correlations. Following this, various model calculations for density distribution, root-mean-square (*rms*) radius of the ground as well as excited state have been performed for different nuclei,

namely ${}^4\text{He}$, ${}^{16}\text{O}$, ${}^{40}\text{Ca}$, etc. The method has been used for evaluating the scaling function by using Fermi gas in relativistic mode [52], and comparing with the results implemented on lepton-scattering processes [52–54]. This scaling function can be used for predicting possible cross-sections for various processes, namely neutrino or antineutrino scattering, for varying charges and neutral-current [53, 54], electron scattering in the δ - as well as quasi-elastic regions [53]. Furthermore, in recent years, this model was used for studying the scaling function using its connection to the spectral function and momentum distribution. Thus, this method is used to formulate different characteristics of nuclear matter, namely symmetry energy, neutron pressure, etc. There are many advantages of using the CDFM approach: firstly, it fends for the fluctuations observed in the density distribution via. weight function $|\mathcal{F}(x)|^2$. Secondly, it can also take care of changes observed in the density and momentum distributions in finite nuclei near the surface. Recently Bhuyan *et al.* have successfully studied various surface properties like symmetry energy, neutron pressure, skin thickness etc., of some exotic finite nuclei using the CDFM within RMF formalism [45].

In CFDM one can define the one-body density matrix (OBDM) $\rho(\mathbf{r}, \mathbf{r}')$ which can take the form of another OBDM having coherent superposition $\rho_x(\mathbf{r}, \mathbf{r}')$ for spherical pieces of NM called as fluctons.

$$\rho_x(\mathbf{r}) = \rho_0(x)\Theta(x - |\mathbf{r}|), \quad (2.21)$$

Here $\rho_0(x) = \frac{3A}{4\pi x^3}$. Moreover, x is defined as the spherical generator radius coordinate for mass number A which lies inside the uniform spherical distribution of Fermi gas. In the case of finite system, OBDM becomes

$$\rho(\mathbf{r}, \mathbf{r}') = \int_0^\infty dx |\mathcal{F}(x)|^2 \rho_x(\mathbf{r}, \mathbf{r}'). \quad (2.22)$$

Here $|\mathcal{F}(x)|^2$ is defined as the weight function while $\rho_x(\mathbf{r}, \mathbf{r}')$ represents the superposition of the OBDM coherently and is stated as:

$$\rho_x(\mathbf{r}, \mathbf{r}') = 3\rho_0(x) \frac{J_1(k_F(x)|\mathbf{r} - \mathbf{r}'|)}{(k_F(x)|\mathbf{r} - \mathbf{r}'|)} \times \Theta\left(x - \frac{|\mathbf{r} + \mathbf{r}'|}{2}\right).$$

The term J_1 is a Bessel function having order as one and $k_F(x)$ represents nucleons Fermi momentum having x radius for the flucton stated as

$$k_F(x) = \left(\frac{3\pi^2}{2} \rho_0(x) \right)^{1/3} \equiv \frac{\beta}{x} \quad (2.23)$$

with

$$\beta = \left(\frac{9\pi A}{8} \right)^{1/3} \simeq 1.52A^{1/3}. \quad (2.24)$$

We can write the Wigner distribution function for the OBDM as

$$W(\mathbf{r}, \mathbf{k}) = \int_0^\infty dx |\mathcal{F}(x)|^2 W_x(\mathbf{r}, \mathbf{k}). \quad (2.25)$$

where $W_x(\mathbf{r}, \mathbf{k}) = \frac{4}{8\pi^3} \Theta(x - |\mathbf{r}|) \Theta(k_F(x) - |\mathbf{k}|)$ Similarly using CDFM approach the density $\rho(r)$ term can be written as,

$$\begin{aligned} \rho(r) &= \int d\mathbf{k} W(\mathbf{r}, \mathbf{k}) \\ &= \int_0^\infty dx |\mathcal{F}(x)|^2 \frac{3A}{4\pi x^3} \Theta(x - |\mathbf{r}|) \end{aligned} \quad (2.26)$$

and weight function $|\mathcal{F}(x)|^2$ as

$$|\mathcal{F}(x)|^2 = - \left(\frac{1}{\rho_0(x)} \frac{d\rho(r)}{dr} \right)_{r=x}, \quad (2.27)$$

having normalization $\int_0^\infty dx |\mathcal{F}(x)|^2 = 1$.

Following the CDFM approach and using the Refs. [45, 55, 55–57], the expression for effective symmetry energy S can be written as:

$$S = \int_0^\infty dx |\mathcal{F}(x)|^2 S^{NM}(x). \quad (2.28)$$

2.4 Developing the Fortran program

The most challenging part of this project work involved writing a program from scratch. We chose Fortran as the programming language for this task because of its superiority in

environments dealing with extreme computations. Fortran as a programming language was invented by J. W. Backus in the 1950s for simplifying scientific and engineering problems. It has stood the test of time for nearly the past six decades by dominating in the different domains, namely computational physics, numerically performed weather prediction, computational-fluid dynamics, etc.

The procedure and hindrance faced while writing the program can be summarized as follows:

- In the initial phase, we have the density file obtained from solving RMF equations with NL3 and DD-ME2 parameters.

- We need this density file to serve as an input to the Fortran program. This density file contains density (ρ) as a function of nuclear distance (r) arranged in different columns. We input these values of nuclear distances and densities to save them in different arrays.

- Using these density values, we calculate the spherical fluctons densities and also save them in the form of arrays.

- Moreover, we perform the numerical derivative operation on densities using the central difference formula using these same densities. Here we create a subroutine for differentiation operation to facilitate handling such a large chunk of data.

- After getting our hands on fluctons densities as well as derivative of densities, we proceed with the calculation of $|\mathcal{F}(x)|^2$ using the CDFM approach.

The equation of $|\mathcal{F}(x)|^2$ may seem to be of simple nature, but on careful observation, it was found that it correlates the infinite nuclear matter quantities in momentum space to that of the finite nuclear system in coordinate space.

The Fortran program for calculation of weight function $|\mathcal{F}(x)|^2$ is provided here. All the variable names have their usual meaning, as discussed in Sec. 2.3.

```
!!!! Program created by Praveen Kumar Yadav
!!!                               M.Sc. Physics
!!! Thapar Institute of Engineering and Technology,
```

```
!!!                Patiala, India

program main
implicit none

integer*8 i, j, n
real*8, dimension(900) :: r, Pn, Pp, Pt
real*8, dimension(900) :: x, Px
real*8 diff_value, h

real*8 pi, massno
real*8, dimension(900) :: p0x, Pt_diff, Fx2
pi=3.141592653589793238
n=299

print *, 'Input_Mass_No_for_data_file'
read(*,*) massno
open(unit=11,file='file.dat', status='old')
do i = 1, n
read(11,*) r(i), Pn(i), Pp(i), Pt(i)
end do
close(11)

h=r(2)-r(1)
do i=2,n-1
j=i-1
call diff_subr(Pt,i,h,diff_value)
Pt_diff(j)=diff_value
end do

do j=1,n-2
x(j)=r(j+1)
```


Chapter 3

Results and discussions

In the relativistic mean-field theory, the mesons are collectively represented as fields, where they account for the interactions between the nucleons. Using the RMF theory, we solve self-consistently various mean-field equations by taking different sets of deformations in the form of input. Following the method of CDFM, which is discussed in section 2.3, we calculate the value of $\mathcal{F}(x)^2$ by the use of different nuclear densities. One of the CDFM's primary benefits is its ability to form transparent relationships for the intrinsic EOS values analytically by using a simple technique related to weight function. Moreover, we calculate the values of nuclear symmetry energy for Scandium ($Z=21$) and Titanium ($Z=22$) isotopic chains. The equation discussed in section 2.3 correlates the infinite nuclear matter (INM) quantities lying in momentum space to its corresponding finite matter system (FNS) quantity existing in coordinate space. Using this weight function, we calculate the value of surface properties of finite nuclei. In our preliminary results, we have calculated the weight function as well as symmetry energy for the finite isotopic chain of *Sc*- and *Ti*- nuclei. These preliminary results based on our calculations are given below.

3.1 Densities and weight function

In order to calculate symmetry energy, the first step is to take the total density as the input to the program. The value of total density is given as the sum of both the neutron density (ρ_n) and the proton density (ρ_p). After getting the value of total densities as a function of nuclear distance, we use the coherent density fluctuation method (CDFM)

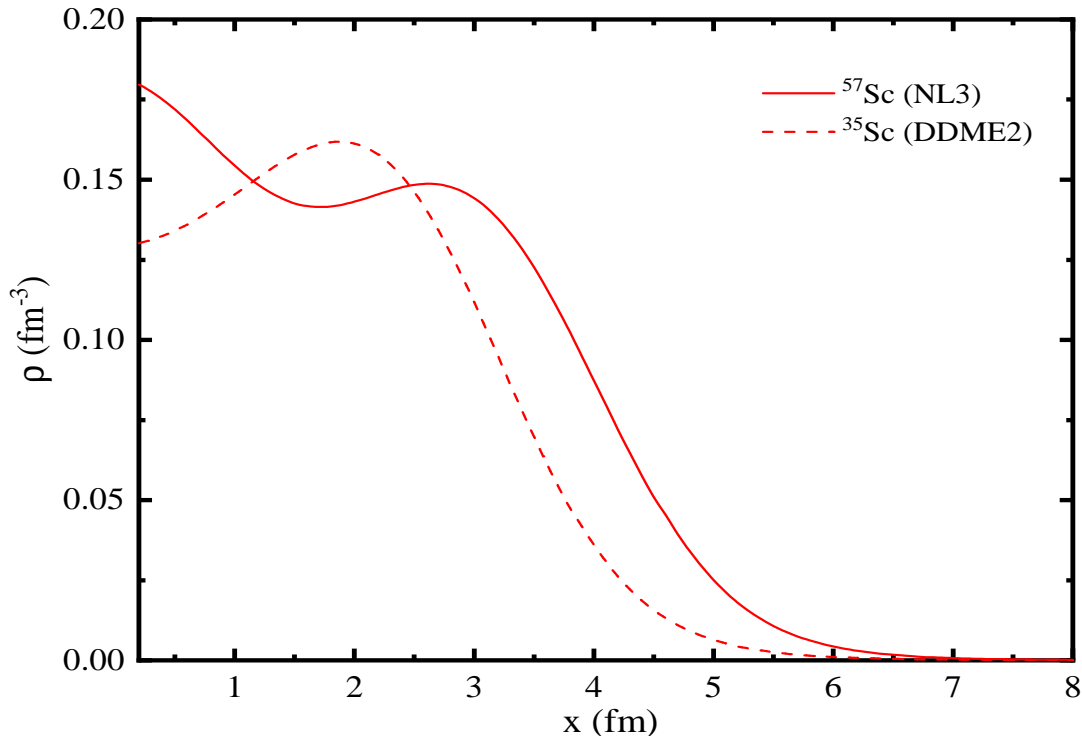


Figure 3.1: Total density distribution for $^{57}\text{Sc}(\text{NL3})$ and $^{35}\text{Sc}(\text{DDME2})$ isotopes.

to evaluate the value of weight function $\mathcal{F}(x)^2$ from Eq. 2.27. The equation of weight function $\mathcal{F}(x)^2$ may appear to be of simple nature but holds an entirely complex interpretation in the realm of nuclear-astronomy. The term $\mathcal{F}(x)^2$ correlates quantities related to INM that exist in momentum space to that of coordinate space found in FNS.

After calculating $\mathcal{F}(x)^2$, we generate the value of symmetry energy using the Eq. 2.28. It must be noted that the value of the $\mathcal{F}(x)^2$ is always less than one. In the Figs. 3.1 and 3.2, we have plotted the graph of total density (ρ) of some *Sc* and *Ti* isotopes with respect to nuclear distance (x). A careful investigation of these Figs. 3.1 and 3.2 suggest that with the increasing number of protons (Z), minor enhancement can be observed in the surface region. Therefore, the total density distribution plays a vital role in understanding various effective nuclear matter quantities.

We have plotted the graph of $\mathcal{F}(x)^2$ as a function of nuclear distance in Fig. 3.3 and 3.4. As can be seen from the graphs, the term $\mathcal{F}(x)^2$ is directly dependent on the density function. Any decrement in the value of density leads to a corresponding decrease in the value of $\mathcal{F}(x)^2$. The shape taken by $\mathcal{F}(x)^2$ corresponds to a bell-shaped structure with a maximum-density value is obtained at the middle of the flucton radius.

Using the $\mathcal{F}(x)^2$ we take the limits of integration corresponding to the symmetry

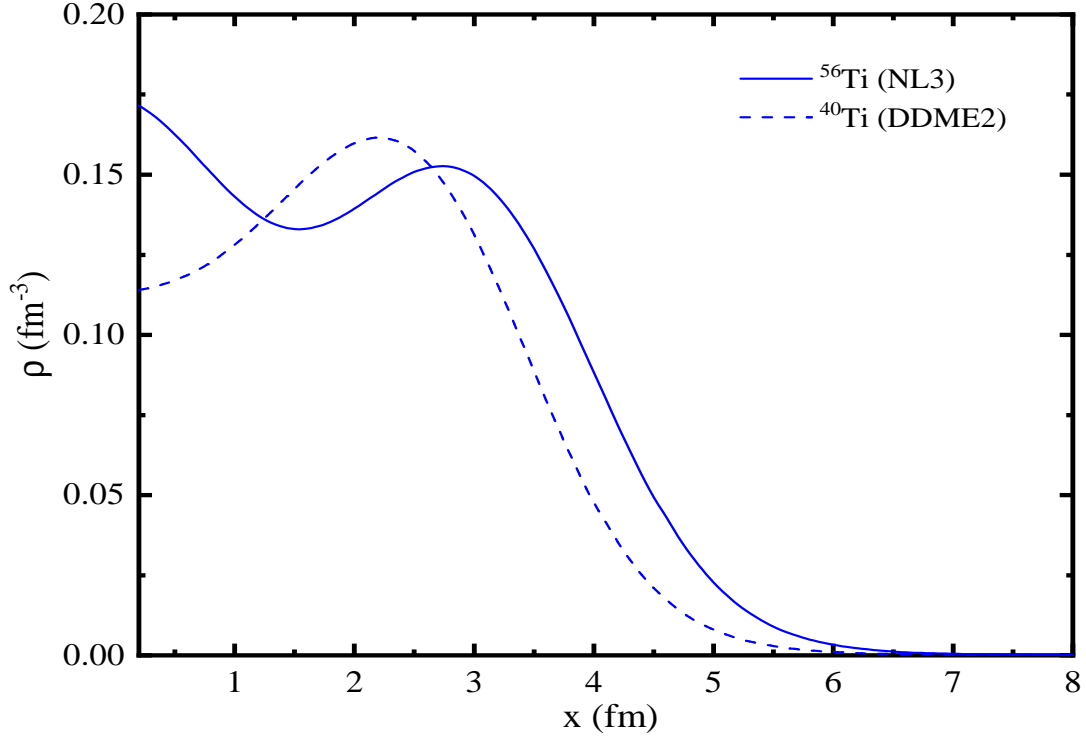


Figure 3.2: Total density distribution for $^{56}\text{Ti}(\text{NL3})$ and $^{40}\text{Ti}(\text{DDME2})$ isotopes

energy in such a way that to only account for the positive value of the product of $\mathcal{F}(x)^2$ and $S^{NM}(x)$. This is done owing to the non-negative nature of NSE. On careful observation, one can note that a considerable portion of the $\mathcal{F}(x)^2$ achieves its peak for the range that corresponds to the density distribution of its surface region. Thus, it is called effective surface properties of finite nuclear matter.

3.2 Nuclear symmetry energy

The main objective of this project involves calculating NSE for nuclei corresponding to two chains of isotopes, namely Scandium and Titanium. NSE is a very important term that has its roots in various branches of nuclear physics, for example, in studying the structure of ground state nuclei, dynamics related to heavy-ion reactions, as well as the composition of neutron stars. Because of the high importance of symmetry energy, its characterization plays a vital role in interpreting neutron-rich nuclei and neutron star matter. The isospin asymmetry in nuclear matter arises due to the differences in densities and masses of protons and neutrons. It helps in the determination of the symmetry energy parameter. Symmetry energy can be defined as the energy density derivative with respect to the

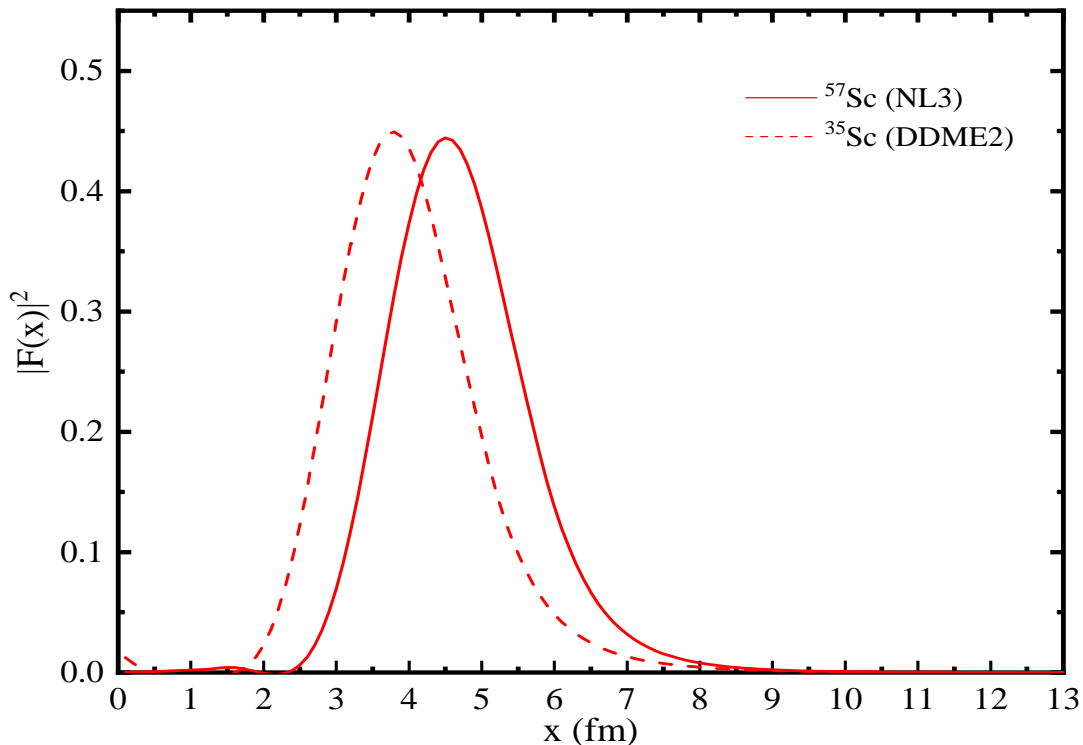


Figure 3.3: The weight function distribution calculated for $^{57}\text{Sc}(\text{NL3})$ and $^{35}\text{Sc}(\text{DDME2})$ isotopes.

isospin asymmetry. Even though it is impossible to measure symmetry energy directly, we can infer its values by using other nuclear observables that share some mathematical relationship with it.

Using the symmetry energy, we can calculate the surface symmetry energy as well as volume symmetry energy. For lighter nuclei, it can be observed that the surface effects are very significant, whereas in the case of heavier nuclei, they provide a negligible contribution. It is possible to consider the effects of deformation during the calculation process for more accurate results. However, this addition of deformation raises the complexity and requires a tremendous amount of computation. Therefore, in our present calculations, we include only the spherical densities.

The NSE is divided into volume and surface components that are generally estimated in relation to the properties of nuclear matter at saturation. According to Brueckner's energy density functional method, few of the negative values of NSE, which are non-physical, were observed. Thus, it is required to define proper limits of integration in the Eq. 2.28 that is based on $S^{NM}(x)$, where it changes sign from a negative to a positive value and vice-versa, respectively.

It must be noted that, in Eq. 2.28 we have defined x_{max} based on the right part of

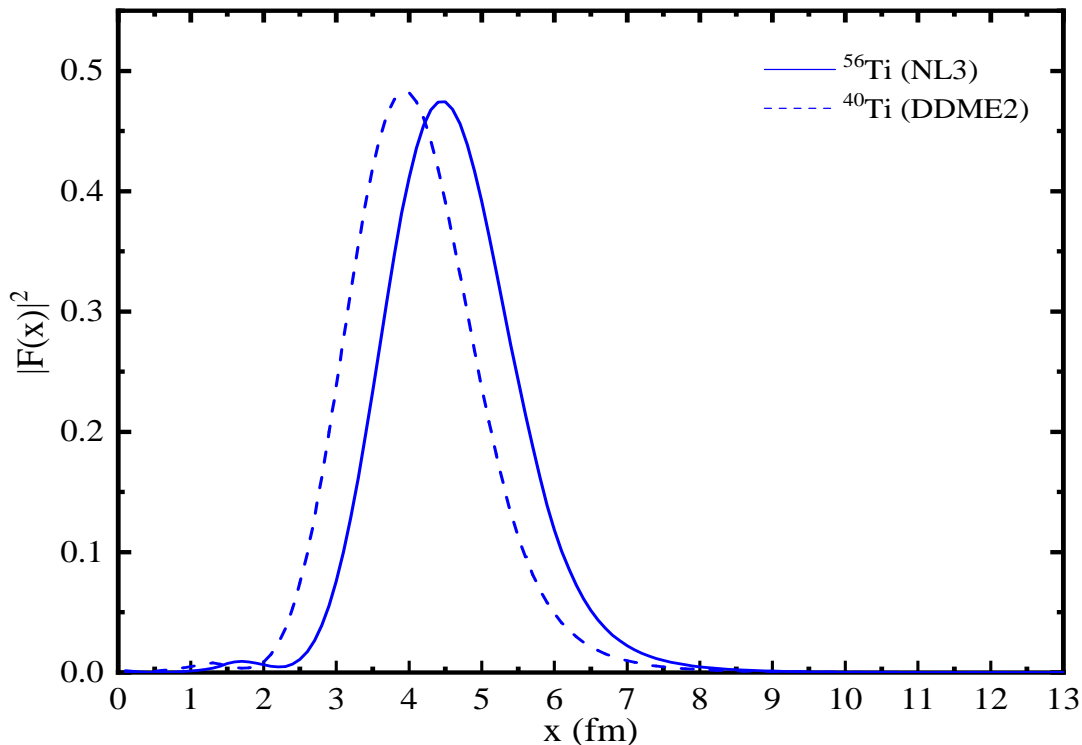


Figure 3.4: The weight function distribution calculated for ^{56}Ti (NL3) and ^{40}Ti (DDME2) isotopes.

the weight function $|\mathcal{F}(x)|^2$. Thus, the integration of S terms from x_{max} to ∞ becomes nearly equal to zero.

Exotic nuclei with significant neutron-proton asymmetry correspond to NSE. In addition to this, relevant symmetry energy information from finite nuclei gets included in different nuclear phenomena, ranging from the nuclear structure study and heavy-ion collision dynamics to large isospin asymmetric systems like neutron stars.

The results of our present calculations related to symmetry energy are displayed in Fig. 3.5 and 3.6. These figures correspond to calculations based on non-linear NL3 and density-dependent DDME2 parameters for Sc- and Ti- isotopes. From the Fig. 3.5 and 3.6 one can find sharp discontinuities, which marks the existence of shell/ sub-shell closure taking place at neutron numbers $N = 20$ and 28 . We know that $N = 20$ and 28 correspond to magic numbers that have a higher degree of nuclear stability. Therefore, these nuclei, which have a magic shell configuration, would require a greater amount of energy in order for a proton to be converted into a neutron or in the other way from neutron to proton. The validity of our calculation is thus confirmed, as we provide theoretical confirmation of the existence of shell and or sub-shell closure for these isotopic chains, which have magic number configurations. Moreover, for both the Sc and Ti isotopic chains, we observe

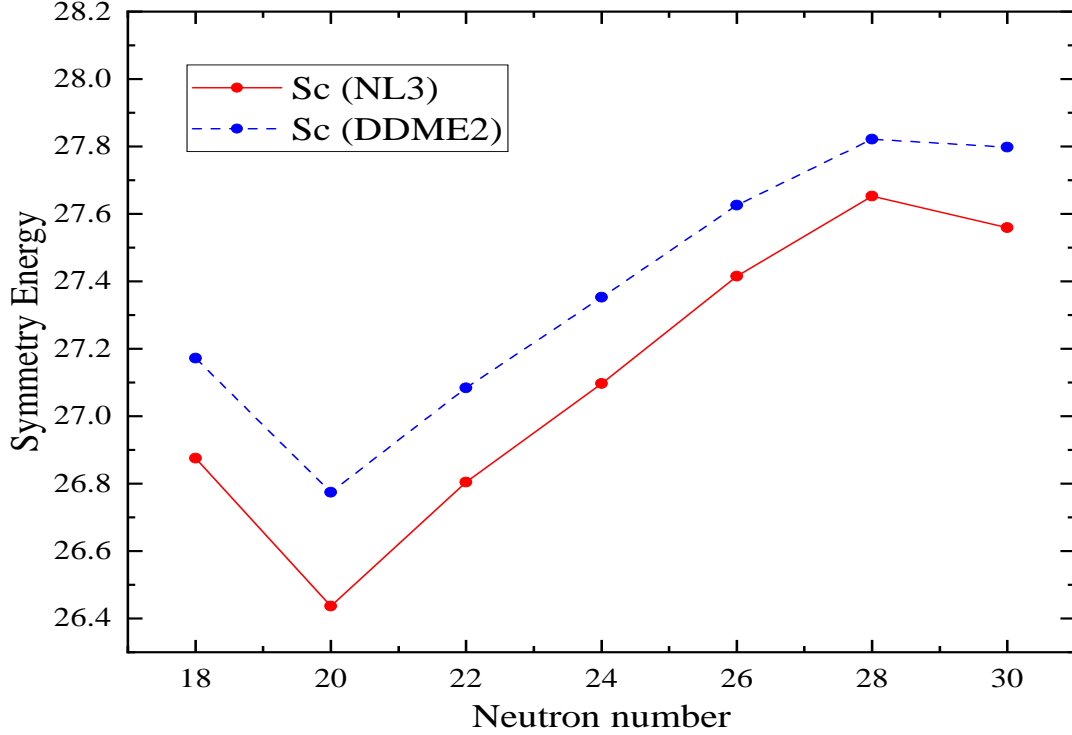


Figure 3.5: The symmetry energy for Scandium isotopes with respect to neutron number for the NL3 and DD-ME2 interactions. More details are provided in the text.

that the DDME2 parameter has a larger value in comparison to the much older NL3 parameter set. This reveals that the contribution of the surface is greater in the DDME2 parameter than in case of the NL3 parameter set.

The symmetry energy values obtained from Sc- isotopic nuclei for NL3 are in the range of $26.43 \leq S \leq 27.65$ while for DDME2 it lies in the range of $26.77 \leq S \leq 27.82$. Moreover, the calculated values from Ti chain and NL3 parameter are found to be between $26.54 \leq S \leq 27.87$ while in case of DDME2 it lies between $26.86 \leq S \leq 28.02$.

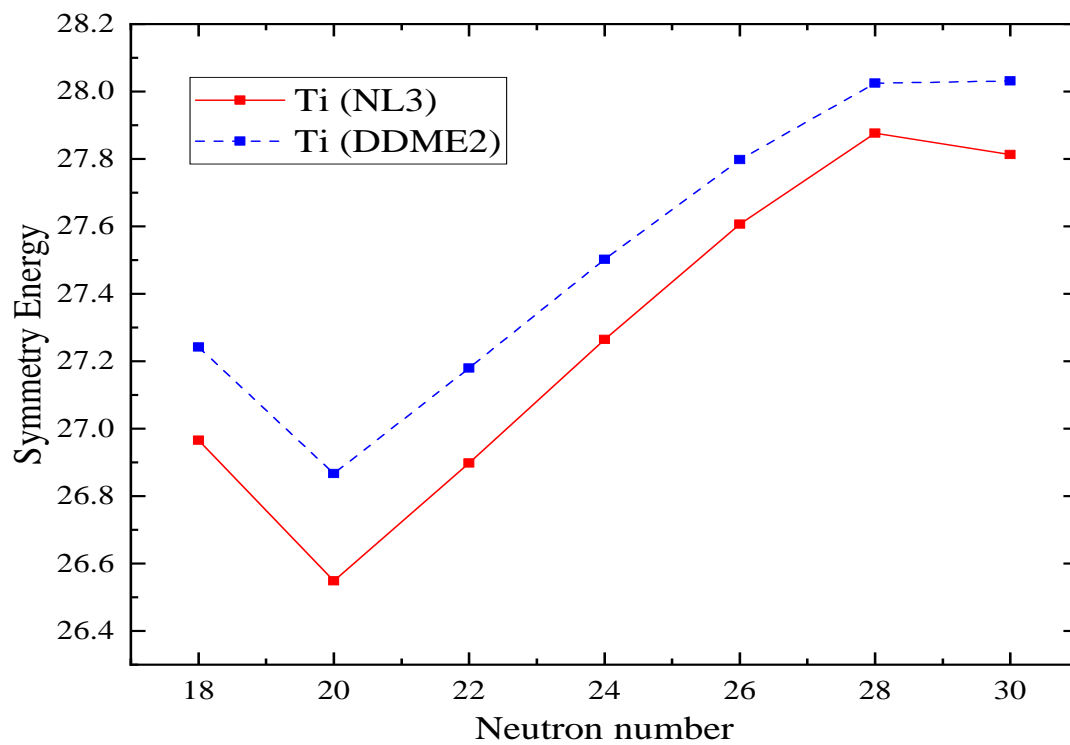


Figure 3.6: The symmetry energy for Titanium isotopes as a function of number of neutrons for the NL3 and DD-ME2 parameters. Detailed explanation is provided in the text.

Chapter 4

Summary and conclusions

4.1 Brief summary

This dissertation attempts to investigate two parameter sets, namely non-linear NL3 and density-dependent DD-ME2, within the purview of relativistic mean-field formalism. We have used the coherent density fluctuation method to find shell/sub-shell closure for the isotopic chains of Scandium and Titanium nuclei. A short chapter-wise summary of this dissertation is given below:

Chapter 1: The chapter briefly deals with the theory of nuclear matter. It includes the topic related to understanding the drip-line nuclei, such as the valley of β -stability, the concept of magic numbers, exotic and halo nuclei, and the role of nuclear deformations. Furthermore, it includes the introduction of relativistic mean-field model and its need and superiority over other types of non-relativistic mean-field models. It also briefly discusses the idea of effective field theory and infinite nuclear matter.

Chapter 2: This chapter deal with the detailed formalism of RMF along with the related equations. A brief description of different mesons, along with the approximations related to the meson field, is detailed in this chapter. Moreover, it also discusses two of the most critical parts of this dissertation: understanding the coherent density fluctuation method and writing the complex Fortran code from scratch. It highlights all the methods used throughout the code creation process along with all the hindrances faced. Moreover, we have also provided the Fortran program capable of calculating weight function $\mathcal{F}(x)|^2$ for easier understanding.

Chapter 3: The calculation for finite nuclear isotopic nuclei of Scandium as well as Titanium is provided here. We have first calculated the densities of spherical fluctons and using that we evaluate the value of weight functions. The plot of different densities and their weight functions decide the integration limits of NSE. The symmetry energy is defined as the derivative of energy density with respect to the asymmetry observed in neutrons and protons. We have predicted some shell and or sub-shell closure for nuclei having neutron numbers $N = 20$ and 28 in the case of exotic Scandium and Titanium isotopic chain. These shell/subshell closure depicts magic shell configuration in nuclei which yields to increased stability. Moreover, these stable nuclei would require a greater amount of energy in order to get converted from proton to neutron or vice-versa than their counterparts.

4.2 Future scope of the project

The ultimate objective of nuclear physicists is to define with extreme precision the magicity of various drip-line nuclei. Many experimental researcher groups around the world have made significant advancements in terms of studying the various properties of these drip-line nuclei. Moreover, different theoretical models have also been defined to better predict the experimentally observed results.

Our preliminary results used the relativistic mean-field model and studied light to medium mass nuclei of Scandium and Titanium. We have calculated the weight function and the symmetry energy for these nuclei. In the future, we would like to extend our present calculations to other light, heavy and super-heavy nuclei and figure out the trend in the shell or sub-shell closure near the drip-line.

Moreover, we wish to further our calculations by calculating our parameters such as neutron pressure, curvature, volume symmetry energy, and surface symmetry energy. It is possible to modify the present form of relativistic mean-field equations to account for the deformations, which, even though it increases the complexity, leads to a lowering of error and thus provides better results. We intend to include more parameter sets and compare them with the experimentally available data along with different theoretical models such as the finite range droplet model and Hartree-Fock plus Bardeen-Cooper-Schrieffer.

Bibliography

- [1] K. L. Jones and W. Nazarewicz, *The Phys. Teacher* **48**, 381 (2010).
- [2] P. Ring, *Prog Part Nucl Phys* **37**, 193 (1996).
- [3] H. Sakurai, *Nucl. Phys. A* **805**, 526c (2008).
- [4] M. Thoennessen, *Nucl. Phys. A* **834**, 688c (2010).
- [5] C. J. Gross *et al.*, *Nucl. Instr. Methods A*, **450**, 12 (2000).
- [6] M. Leino *et al.*, *Nucl. Instrum. Methods Phys. Res. B* **99**, 653 (1995).
- [7] M. Winkler *et al.*, *Nucl. Instrum. Methods Phys. Res. B* **266**, 4183 (2008).
- [8] H. Geissel *et al.*, *Nucl. Instrum. Methods Phys. Res. B* **70**, 286 (1992).
- [9] Z. Sun, W. L. Zhan, Z. Y. Guo, G. Xiao, and J. X. Li, *Nucl. Instrum. Methods Phys. Res., A* **503**, 496 (2003).
- [10] A. C. Mueller and R. Anne, *Nucl. Instrum. Methods Phys. Res. B* **56-57**, 559 (1991).
- [11] A. M. Rodin *et al.*, *Nucl. Instrum. Methods Phys. Res. B* **204**, 114 (2003).
- [12] S. M. Lukyanov *et al.*, *J. Phys. G: Nucl. Part. Phys.* **28**, L41 (2002).
- [13] M. Notani *et al.*, *Phys. Lett. B* **542**, 49 (2002).
- [14] T. Baumann *et al.*, *Nature* **449**, 1022 (2007).
- [15] R. K. Gupta, S. K. Patra, and W. Greiner, *Modern Phys. Lett. A* **12**, 1727 (1997).
- [16] T. Otsuka, R. Fujimoto, Y. Utsuno, B. A. Brown, M. Honma, and T. Mizusaki, *Phys. Rev. Lett.* **87**, 082502 (2001).
- [17] T. Otsuka, T. Suzuki, M. Honma, Y. Utsuno, N. Tsunoda, K. Tsukiyama, and M. Hjorth-Jensen, *Phys. Rev. Lett.* **104**, 012501 (2010).
- [18] I. Tanihata *et al.*, *Phys. Rev. Lett.* **55**, 2676 (1985).

- [19] I. Tanihata, T. Kobayashi, O. Yamakawa, S. Shimoura, K. Ekuni, K. Sugimoto, N. Takahashi, T. Shimoda, and H. Sato, *Phys. Lett. B* **206**, 592 (1988).
- [20] C. Détraz *et al.*, *Phys. Rev. C* **19**, 164 (1979).
- [21] C. R. Hoffman *et al.*, *Phys. Rev. Lett.* **100**, 152502 (2008).
- [22] P. Doornenbal *et al.*, *Phys. Rev. Lett.* **103**, 032501 (2009).
- [23] E. Sahin *et al.*, *Phys. Rev. C* **91**, 034302 (2015).
- [24] P. Möller, A. J. Sierk, T. Ichikawa, and H. Sagawa, *At. Data. Nucl. Data Tables* **109-110**, 1 (2016).
- [25] E. Chabanat, P. Bonche, P. Haensel, J. Meyer, and R. Schaeffer, *Nucl. Phys. A* **627**, 710 (1997).
- [26] J. R. Stone and P.-G. Reinhard, *Prog. Part. Nucl. Phys.* **58**, 587 (2007).
- [27] M. Del Estal, M. Centelles, X. Viñas, and S. K. Patra, *Phys. Rev. C* **63**, 044321 (2001).
- [28] Y. K. Gambhir, P. Ring, and A. Thimet, *Ann. Phys.* **198**, 132 (1990).
- [29] M. Bender and P.-H. Heenen, *Phys. Rev. C* **78**, 024309 (2008).
- [30] J. P. Ebran, A. Mutschler, E. Khan, and D. Vretenar, *Phys. Rev. C* **94**, 024304 (2016), arXiv:1607.06567 [nucl-th] .
- [31] R. Brockmann and R. Machleidt, *Phys. Rev. C* **42**, 1965 (1990).
- [32] J. D. Walecka (Springer US, Boston, MA, 1986) pp. 229–271.
- [33] E. M. Burbidge, G. R. Burbidge, W. A. Fowler, and F. Hoyle, *Rev. Modern Phys.* **29**, 547 (1957).
- [34] A. G. W. Cameron, *Publ. Astron. Soc. Pac.* **69**, 201 (1957).
- [35] J. Boguta and A. R. Bodmer, *Nucl. Phys. A* **292**, 413 (1977).
- [36] P.-G. Reinhard, *Rep. on Prog. in Phys.* **52**, 439 (1989).

- [37] M. M. Sharma, G. A. Lalazissis, and P. Ring, *Phys. Lett. B* **317**, 9 (1993).
- [38] G. A. Lalazissis, J. König, and P. Ring, *Phys. Rev. C* **55**, 540 (1997).
- [39] L. I. Schiff, *Phys. Rev.* **84**, 1 (1951).
- [40] M. H. Johnson and E. Teller, *Phys. Rev.* **98**, 783 (1955).
- [41] H.-P. Duerr and E. Teller, *Phys. Rev.* **101**, 494 (1956).
- [42] J. D. Walecka, *Ann. Phys. (NY)* **83**, 491 (1974).
- [43] B. D. Serot and J. D. Walecka, *Int. J. Mod. Phys. E* **06**, 515 (1997).
- [44] M. Centelles, M. Del Estal, X. Viñas, and S. K. Patra (Springer Netherlands, Dordrecht, 2002) pp. 97–102.
- [45] M. Bhuyan, B. V. Carlson, S. K. Patra, and S.-G. Zhou, *Phys. Rev. C* **97**, 024322 (2018).
- [46] B. V. Carlson and D. Hirata, *Phys. Rev. C* **62**, 054310 (2000).
- [47] G. A. Lalazissis, S. Karatzikos, R. Fossion, D. P. Arteaga, A. V. Afanasjev, and P. Ring, *Phys. Lett. B* **671**, 36 (2009).
- [48] T. Nikšić, D. Vretenar, P. Finelli, and P. Ring, *Phys. Rev. C* **66**, 024306 (2002).
- [49] H. A. Bethe and R. F. Bacher, *Rev. Mod. Phys.* **8**, 82 (1936).
- [50] W. Pannert, P. Ring, and J. Boguta, *Phys. Rev. Lett.* **59**, 2420 (1987).
- [51] S. Goriely, F. Tondeur, and J. M. Pearson, *At. Data. Nucl. Data Tables* **77**, 311 (2001).
- [52] A. N. Antonov, M. K. Gaidarov, D. N. Kadrev, M. V. Ivanov, E. Moya de Guerra, and J. M. Udias, *Phys. Rev. C* **69**, 044321 (2004).
- [53] M. V. Ivanov, M. B. Barbaro, J. A. Caballero, A. N. Antonov, E. M. d. Guerra, and M. K. Gaidarov, *Phys. Rev. C* **77**, 034612 (2008).
- [54] A. N. Antonov, M. V. Ivanov, M. B. Barbaro, J. A. Caballero, and E. M. de Guerra, *Phys. Rev. C* **79**, 044602 (2009).

- [55] A. N. Antonov, D. N. Kadrev, and P. E. Hodgson, *Phys. Rev. C* **50**, 164 (1994).
- [56] M. K. Gaidarov, A. N. Antonov, P. Sarriguren, and E. Moya de Guerra, *Phys. Rev. C* **84**, 034316 (2011).
- [57] P. Sarriguren, M. K. Gaidarov, E. M. d. Guerra, and A. N. Antonov, *Phys. Rev. C* **76**, 044322 (2007).

Turnitin Originality Report

Processed on: 18-Jul-2021 15:49 +0530

ID: 1620959869

Word Count: 8097

Submitted: 1

Similarity Index	Similarity by Source
8%	Internet Sources: 2%
<i>Raj Kumar</i>	Publications: 7%
	Student Papers: 1%

Praveen Thesis By Praveen Yadav

1% match ()

[Quddus, Abdul, Bhuyan, M., Patra, S. K.. "Effective surface properties of light, heavy, and super-heavy nuclei", 'IOP Publishing', 2019](#)

1% match (publications)

[P. Ring. "Relativistic mean field theory in finite nuclei", Progress in Particle and Nuclear Physics, 1996](#)

1% match (publications)

[Bharat Kumar, S. K. Patra, B. K. Agrawal. "New relativistic effective interaction for finite nuclei, infinite nuclear matter, and neutron stars", Physical Review C, 2018](#)

< 1% match (publications)

[S.K. Biswal, M.K.Abu El Sheikh, N. Biswal, N. Yusof, H.A. Kassim, M. Bhuyan. "Nuclear matter properties of finite nuclei using relativistic mean field formalism", Nuclear Physics A, 2020](#)

< 1% match (publications)

[Abdul Quddus, M. Bhuyan, Shakeb Ahmad, B. V. Carlson, S. K. Patra. "Temperature-dependent symmetry energy of neutron-rich thermally fissile nuclei", Physical Review C, 2019](#)

< 1% match (publications)

[M. K. Gaidarov, A. N. Antonov, P. Sarriguren, E. Moya de Guerra. "Surface properties of neutron-rich exotic nuclei: A source for studying the nuclear symmetry energy", Physical Review C, 2011](#)

< 1% match (student papers from 24-Dec-2015)

[Submitted to Thapar University, Patiala on 2015-12-24](#)

< 1% match (publications)

[M. Bhuyan, S. K. Patra, B. V. Carlson. "Infinite nuclear matter characteristics of the finite nuclei within relativistic mean-field formalism", Astronomische Nachrichten, 2019](#)

< 1% match (publications)

["Handbook of Nuclear Chemistry", Springer Nature, 2011](#)

< 1% match (publications)

[Khalaf Gad, Hesham Mansour. "Equation of State and Symmetry Energy at High Densities for Zero and Finite Temperatures", Journal of the Physical Society of Japan, 2015](#)

Kumar